

An Evaluation of Visual Interfaces for Teleoperated Control of Kinematically Redundant Manipulators*

Shantell R. Hinton, Randy C. Hoover, and Anthony A. Maciejewski

Dept. of Electrical and Computer Eng.

Colorado State University

Fort Collins, CO 80523-1373, USA

Email: {hintons,hoover,aam}@engr.colostate.edu

Abstract

The utilization of robots in hazardous environments for tasks that require high safety and/or precision is significantly increasing. In this work, we consider scenarios where kinematically redundant manipulators are teleoperated to complete tasks specified by point-to-point motion. Teleoperator performance is evaluated based on several different criteria. We build upon previous work on the performance of human/robotic systems by studying the effects of two different visual interfaces. Namely, we compare a world view with an eye-in-hand view and evaluate how these two different visual interfaces affect human performance and task completion.

1 Introduction

Teleoperation has become more widely researched in the last several decades and has been continually improved since its inception [1]. Specifically, teleoperated human/robotic systems have been applied in space exploration [2, 3], underwater navigation [4], and surgical operations [5, 6]. In all cases that use telerobotics, there is always the issue of providing an effective human-robot interface to ensure optimal human performance and successful task completion.

Previous work on teleoperated systems has explored human robot interaction (HRI) and the flow of information between the operator and manipulator [7]. Several issues have been addressed including how to deal with such issues as time delay [8], translation of human movement to robotic movement [5], and transparency of the telerobotic system [9]. Because there are so many different factors that may affect human performance in task achievement, teleop-

eration has been used in simulated environments for learning the capabilities of operators, as well as for training them to perform specific tasks [10]. Computer simulated environments also allow one to easily evaluate different visual interfaces [11].

There are numerous methods to present the user with an accurate representation of the telerobotic system as well as the task. These representations can positively or adversely affect performance, and must take into consideration the robotic manipulator, constraints imposed by the environment as well as the manipulator itself, and tasks to be completed. In many cases, an overall world view of the given workspace of the robotic manipulator, as well as the task at hand, is provided for the user. In many instances however, such as collision or obstacle avoidance, scenarios may arise where the user has commanded the manipulator into a position where the world view has been obstructed by either the robot or another object in the workspace. An alternate method is to provide a view of the workspace as seen by the robotic manipulator's end effector, i.e., an eye in hand view.

In [11], Magenes *et al.* investigate human strategies in teleoperated systems by presenting operators with different visual frames of reference. The manipulator used in [11] had three degrees of freedom (DOF) and the user was given tasks that required maneuvering the end-effector through three-dimensional space to reach a desired location while avoiding known obstacles. If a manipulator has more DOF than the task requires, the manipulator is said to be kinematically redundant. For kinematically redundant manipulators, there is typically more than one solution to satisfy a given task, i.e., the manipulator may be able to reach a particular workspace location from many different orientations. In each task developed in [11], the DOF of the manipulator and the DOF required to complete the task were equivalent, i.e. the manipulator offered no additional DOF and as such was not redundant. As a result, [11] also explored the case where each task had a predetermined trajec-

*This work was supported in part by the National Science Foundation under the Bridge to the Doctorate Program.

tory that the user had to track to accomplish the task while avoiding obstacles.

In the work presented here we build upon [11] by focusing our attention on the comparison of two different visual interfaces and use a redundant manipulator with a single degree of redundancy. The manipulator's workspace is constrained by its physical joint limits. Using a redundant manipulator allows the operator to complete a given task from many different configurations within the workspace while coping with the imposed joint constraints. We then evaluate how both interfaces affect human performance.

The remainder of this paper is organized as follows: In Section 2, we discuss the mathematical framework used to control the kinematically redundant manipulator in the teleoperation environment. In Section 3 a description of the experimental test bed and protocol is explained. In Section 4, an evaluation of the two different interfaces is discussed and an analysis of the results are given. Conclusions and future work are outlined in Section 5.

2 Mathematical Framework

Let the kinematic function mapping the joint space $\mathcal{C} \subset \mathbb{R}^n$ to the workspace $\mathcal{W} \subset \mathbb{R}^m$ be denoted by $\mathbf{f} : \mathcal{C} \rightarrow \mathcal{W}$ where m and n are the dimensions of the workspace and joint space respectively. The location of the manipulator's end-effector is related to its configuration by

$$\mathbf{x} = \mathbf{f}(\mathbf{q}) \quad (1)$$

where $\mathbf{x} \in \mathcal{W}$ is the position of the end-effector, $\mathbf{q} \in \mathcal{C}$ is the vector of joint variables, and $\mathbf{f}(\mathbf{q})$ is defined by the forward kinematics of the manipulator. In point-to-point (PTP) tasks, \mathbf{x}_s and \mathbf{x}_g would represent the start location and goal location of the manipulator's end-effector respectively. The inverse kinematic relationship is then defined by

$$\mathbf{q} = \mathbf{f}^{-1}(\mathbf{x}) \quad (2)$$

which determines the joint configurations required for the manipulator to reach a specified location in the workspace. If a manipulator's joint space is larger than its workspace, i.e., $n > m$, the manipulator is said to be redundant. In redundant manipulators, the number of DOF of the manipulator is larger than the task requires. As a result, (2) may have an infinite number of solutions. Furthermore, because the kinematic mapping $\mathbf{f}(\mathbf{q})$ is nonlinear, there is typically no closed form solution to the inverse problem $\mathbf{f}^{-1}(\mathbf{x})$. As a result, it is common to use velocity (rather than position) based control for teleoperation where the user input is the commanded end-effector velocity.

The relationship between the velocity of the manipulator's end-effector $\dot{\mathbf{x}}$ due to a set of joint velocities $\dot{\mathbf{q}}$ is given by

$$\dot{\mathbf{x}} = J(\mathbf{q})\dot{\mathbf{q}} \quad (3)$$

where $J(\mathbf{q}) \in \mathbb{R}^{m \times n}$ is the manipulator Jacobian, which is a linearization of the forward mapping $\mathbf{f}(\mathbf{q})$ evaluated at the configuration defined by \mathbf{q} . As long as the joint velocities remain "small", this linear approximation remains valid. The inverse problem can then be defined as

$$\dot{\mathbf{q}} = J^+(\mathbf{q})\dot{\mathbf{x}} + \alpha\hat{\mathbf{n}}_J(\mathbf{q}) \quad (4)$$

where, for nonsingular J , $J^+(\mathbf{q}) = J^T(\mathbf{q})(J(\mathbf{q})J^T(\mathbf{q}))^{-1}$ is the pseudo-inverse solution of the manipulator Jacobian, $\hat{\mathbf{n}}_J(\mathbf{q})$ is the null space vector of the manipulator Jacobian (assuming a single degree of redundancy), and the scalar α is chosen to accomplish some secondary task. Some common uses of $\hat{\mathbf{n}}_J(\mathbf{q})$ have been failure tolerance, obstacle avoidance, and dexterity optimization [12–15].

In the current work, we use the addition of the null space vector to help compensate for restricted motion due to a joint limit. When the manipulator's joints are all operating within their pre-defined operating range, the manipulator is free to move in the unconstrained workspace. The joint space velocities in this case are computed using (4) with $\alpha = 0$ and $\dot{\mathbf{q}} = J^+(\mathbf{q})\dot{\mathbf{x}}$, which minimizes the norm of the joint velocity. Unfortunately, when $\alpha = 0$, neither (2) or (4) take into consideration the possibility that a joint has reached its limit. In this case, α is chosen so that (4) compensates for the restricted motion.

3 Description of Experiment

3.1 Experimental Testbed

The manipulator used in the experimental study consists of a three-dimensional (3-D) computer graphic model of a three-DOF planar system. The computer graphic model is based on the Mitsubishi PA-10-7c industrial robot. The manipulator geometry consists of three links of length $L = [0.45, 0.5, 0.5]$ meters. Unlike the actual PA-10, however, the graphical model is restricted to operate in a plane whereas the physical system is a fully spatial seven-DOF manipulator. The joint limits of the computer graphic model are $[\pm 91, \pm 137, \pm 161]$ degrees that correspond to joints 2, 4 and 6 of the PA-10.

In the experimental set-up, velocity control is used to command the manipulator's end-effector to a desired location in the workspace. The robotic manipulator is commanded via user input through a two-dimensional (2-D) joystick. The joystick used in all experiments is a standard commercial self-centering joystick. The joystick input represents a command in end-effector velocity, i.e., $\dot{\mathbf{x}}$ in (4) that is proportional to the joystick's displacement. All graphic models and simulations were performed using MATLAB/SIMULINK on a standard Dell Pentium D computer running Windows XP.

3.2 Task Specification

One can classify tasks in several different ways. In some cases, a pre-defined trajectory is necessary for task completion, e.g., robotic welding or automated spray painting. In other cases, only the start and goal position are important, e.g., pick-and-place tasks [16], where an object is grasped and moved from one set location to the next specified position. This may require maneuvering around objects within the environment to avoid collisions [17]. For this study, we focus on PTP motion, where the robot moves from an initial position to a final position in the workspace.

The tasks used here were derived from a subset of the tasks developed in [18]. Unfortunately, the manipulator used in [18] had a slightly different geometry, as well as an unconstrained workspace. As a result, some of the tasks defined in [18] had to be modified slightly for to guarantee that both the start and goal location are within the reachable workspace. The effect of the joint limit constraints has significant implications on the users ability to reach the desired goal. One such implication is that some tasks defined in [19] which could be completed using a straight line trajectory are no longer achievable (without deviation from the straight line). Another is that fact that even though all goal positions are within the reachable workspace, they are typically not reachable from an arbitrary orientation.

3.3 Testing Procedure

In this study, a group of 12 subjects was tested. The group was comprised of subjects varying in gender, ethnicity, age, and technical background. Because the technical background of all individuals varied, it was assumed that none of the subjects had prior experience using teleoperation. As a result, the subjects were all trained to a specified level of proficiency in using both visual interfaces. The training consisted of tasks in which the user was instructed to command the end-effector from a start location to a goal location using both of the visual interfaces. After the subject was able to complete 5 successive tasks (tasks not used in the experiment) using each interface within a pre-determined time limit, they were deemed proficient in commanding the robot to a specified target. Once a user was deemed proficient, an experimental test task was presented to the subject, and upon completion, the task was rated by the user as to the perceived level of difficulty.

The experiment called for each subject to completed 24 tasks twice, one set of 24 tasks for each of the two different interfaces. The tasks were presented to the user in sequential order, but the first task seen by each user was varied in order to reduce the effect of learning. The first visual interface evaluated in this study consisted of a world view in which the entire workspace, manipulator, and task is seen

by the user from a viewpoint perpendicular to the plane of the robot's operation. The second visual interface consisted of an eye-in-hand view in which the user sees the goal location as seen from a camera mounted near the end effector. This view also provided a cross hair which has the interpretation of the manipulator's end-effector. Both visual interfaces are depicted in Figure 1. The interface on the left of Figure 1 is a depiction of the world view, and the interface on the right is the eye-in-hand view. The world view and the eye-in-hand view are referred to as a stationary environment (SE) and a moving environment (ME), respectively as in [11]. It is important to note, that when using the two different visual interfaces, the perceived motion of the end-effector is different. For the SE interface, the perceived motion is from the manipulator's end-effector to the desired goal, whereas for the ME interface, the cross hairs appear to remain stationary and the perceived motion is the goal moving toward the end-effector.

4 Evaluation of Interfaces and Results

4.1 Measures of Performance

To compare the two different visual interfaces, we use a subset of the performance measures outlined in [18, 19]. The measures pertaining to end-effector velocity error defined in [18, 19] were eliminated in this study because they were motivated by the effects of joint failures which were not considered in this work. Each of these measures is outlined in Table 1. As a means of evaluating the overall performance of a given subject, or the performance of all subject completing a given task, a cumulative performance measure (CPM) is defined as

$$\text{CPM} = \sum_{i=1}^8 \frac{M_i}{\max(M_{i_{ME}}, M_{i_{SE}})}, \quad (5)$$

where $\max(M_{i_{ME}}, M_{i_{SE}})$ corresponds to the maximum value for measure i in both views [19].

4.2 Results

Each of the 12 subjects were capable of completing all 24 tasks in both of the views presented to them. After completing the given tasks, each of the performance measures outlined in Table 1 was computed for each subject in the experiment. The CPM was then computed for each subject as a means of quantifying their performance for a given task using a given visual interface.

Figure 2 shows a plot of the median CPM values for each view sorted by task. This figure illustrates a measure of task difficulty for each view as computed by the CPM. Some key things to note are that some tasks appear to be easier for the

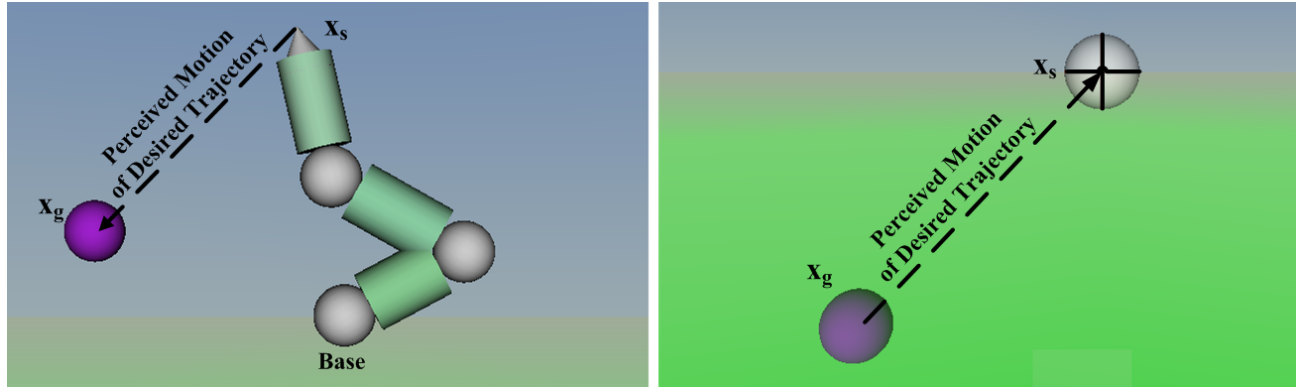


Figure 1. The SE interface is depicted on the left, and the ME interface is depicted on the right. The goal and start locations are labeled as x_g and x_s respectively. Note that when using the SE interface the user sees the end-effector move toward the goal position, however, when using the ME interface the goal is perceived to move toward the end-effector (indicated by the cross hairs).

users to complete depending on the visual interface used. Specifically, subjects performed very poorly on task 23 using the SE interface, however using the ME interface, subjects performed significantly better. The converse of this

is also true for task 1 where on average, the subjects performed much better using the SE interface as opposed to the ME interface. The figure also depicts that certain tasks exist in which performance is comparable using either of the two visual interfaces, e.g. tasks 4 and 21.

Table 1. This table gives a brief description of the performance measures used in this experimental study.

Measure	Description
M_1	<i>Task Completion Time (cycles)</i> (TCT_{cyc}): Computed in terms of the number of controller cycles rather than in elapsed time. Allows control schemes to be evaluated independent of the underlying computational cost.
M_2	<i>Task Completion Time (seconds)</i> (TCT_{sec}): Computed in terms of actual elapsed time.
M_3	<i>Total Path Length (meters)</i> (TPL_m): Total length of end-effector trajectory. Provides measure of total deviation of actual trajectory from ideal straight-line path.
M_4	<i>Peak Trajectory Deviation (mag)</i> (PTD_{mag}): Maximum displacement of end effector from desired straight-line trajectory. Measured over entire task.
M_5	<i>Peak Trajectory Deviation (ang)</i> (PTD_{ang}): Maximum angular deviation of end effector from desired straight-line trajectory.
M_6	<i>Number of Trajectory Corrections</i> (NTC): Corrections made by the operator/computer to compensate for an increase in position error of end effector.
M_7	<i>Excursion of Input Device/Master</i> (EIP): Specific to teleoperation, reflects total effort by an operator while commanding joystick to perform the task.
M_8	<i>Subjective Operator Assessment</i> (SOA): Operator is required to rate the task difficulty with a numeric value from 1-4.

A linear regression was also performed on the data in Figure 2 shown as the solid line. The regression showed that for a similar correlation coefficient (0.9733 for the SE interface and 0.9744 for the ME interface), the slope for the linear fit of the SE data ($m_{SE} = 0.095$) was higher than that for the ME data ($m_{ME} = 0.065$) where m_i corresponds to the slope for interface i . This shows that in general, the SE interface tends to accentuate the difference between easy and difficult tasks, whereas the ME interface tends to even out the relative difficulty between tasks.

An alternate comparison of both visual interfaces based on the measures outlined in Table 1, is to evaluate the ratio of CPM data for one interface versus the other. Figure 3 shows the ratio of the median of the CPM data calculated for each visual interface. In the top plot of Figure 3, the median is taken across all subjects and sorted according to the magnitude of the ratio for each task. In the bottom plot, the median is taken across all tasks and is sorted according to the magnitude of the ratio for each subject. The solid line represents a “break even” point in which according to the performance measures, both visual interfaces are equivalent. A value greater than one indicates that users performed better using the ME interface as opposed to the SE interface. In general, neither interface results in optimal performance for all tasks or for all operators. However, it is obvious that certain tasks are more easily performed with a given interface, e.g., tasks 1 and 23. Likewise, there are operators who perform better given a particular interface, e.g., operator 2

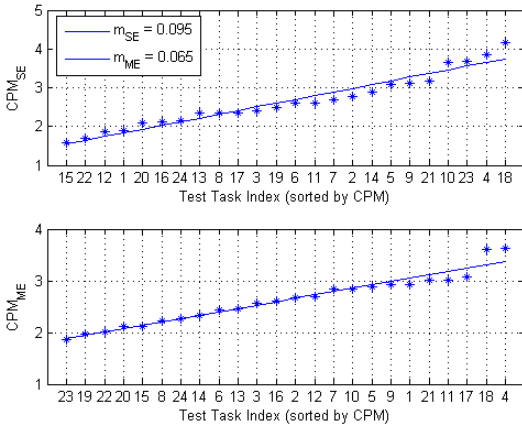


Figure 2. The median CPM value was taken across all 12 subjects for each of the 24 tasks and both views. The tasks are sorted by the task difficulty as measured by the CPM. The solid line shows the linear fit of the data with the slope for each line shown in the legend.

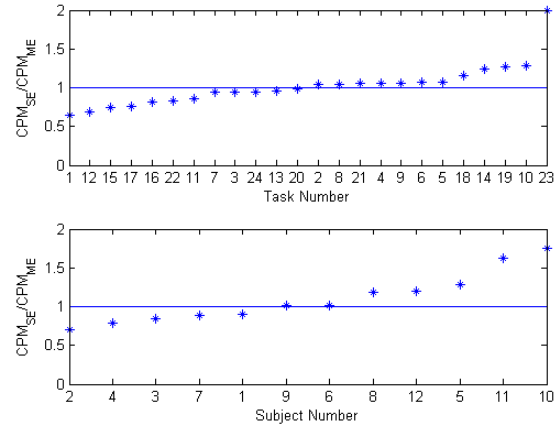


Figure 3. The median CPM value for each view was taken across all 24 tasks [top] and all 12 subjects [bottom]. The horizontal line corresponds to a task/subject in which the performance as measured by the CPM is equivalent for both views.

and 10.

Similar to comparing ratios of CPM data, a subjective assessment can be performed by comparing a ratio of the SOA data for each view. Figure 4 shows the ratio of the median of the SOA data collected for each visual interface. Again, in the top plot of Figure 4, the median is taken across all subjects and sorted according to the magnitude of the ratio for each task. In the bottom plot, the median is taken across all tasks and is sorted according to the magnitude of the ratio for each subject. The solid line in these figures also represent a “break even” point in which subjectively, users felt that they performed equivalently using both visual interfaces. A value greater than one in this figure indicates that users preferred the ME interface as opposed to the SE interface. Note that there is a clear preference for the ME interface in almost all cases.

The contrast between the actual performance of users quantified in Figure 3 as compared to their perception of task difficulty quantified in Figure 4 leads to several interesting observations. One is that although users may prefer one interface over the other, they don’t always perform better using their preference. Therefore, it is not always optimal to allow the user to decide which interface they wish to use for teleoperation. A specific example of this is operator number 7 who clearly prefers the ME interface, however he performed significantly better using the SE interface. This is also evident from the top plots of Figures 3 and 4 in which some tasks appeared to the user to be easier using the ME interface, however according to the performance measures,

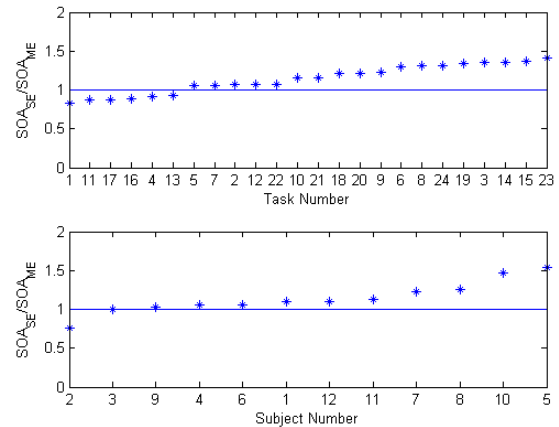


Figure 4. The ratio of the median subjective operator assessment (SOA) value for each view was taken across all 24 tasks [top] and all 12 subjects [bottom]. The horizontal line corresponds to a task/subject in which subjectively, they prefer both views equally.

users actually did better using the SE interface. A specific example of this is task 4.

5 Conclusions and Future Work

This experimental study has presented an evaluation of the effects of offering an operator two different visual interfaces for point-to-point teleoperated tasks. The two visual interfaces used in this study were a world view, SE interface, and an eye-in-hand view, ME interface. The study consisted of 12 subjects performing 24 tasks using each visual interface. We have illustrated that levels of performance are co-dependent upon subjects and tasks. Specifically, some users may have performed very well for a given task using one interface and poorly using the other. Conversely, there are also tasks in which operator performance appears to be independent of interface. While some operators may prefer using one interface rather than the other, operator perception is often not an accurate way of ensuring the best performance in a given task. In addition, operator preference cannot be related to how well one will perform in either of the visual interfaces. We conclude that there is no way to classify one interface as better than the other for all tasks. However, we find advantages and disadvantages between the two visual interfaces that are task-dependent. We also found that manipulator joint limits play a significant role in the user's ability to perform the task within the constrained workspaces. Considering these findings, future work will focus on validating our results on a physical system, as well as providing the user with visual cues indicating the workspace boundary.

References

- [1] E. Johnsen and W. Corliss, *Human Factors Applications in Teleoperator Design and Operation*. New York, NY: Wiley-Science, 1971.
- [2] B. Hannaford, A. Bejcy, P. Buttolo, M. Moreyra, and S. Venema, "Mini-teleoperation technology for space research," in *Proc. of MIMR-95*, Sendai, Japan, Sept. 1995.
- [3] G. Hirzinger, B. Brunner, K. Landzettel, N. Sporer, J. Butterfab, and M. Schedl, "Space robotics - DLR's telerobotic concepts lightweight arms and articulated hands," *Autonomous Robots*, vol. 14, pp. 127–145, 2003.
- [4] Q. Lin and C. Kuo, "A virtual environment-based system for the navigation of underwater robots," *Virtual Reality*, vol. 3, pp. 267–277, 1998.
- [5] G. H. Ballantyne, "Robotic Surgery, Telerobotic Surgery, Telepresence, and Telementoring," *Surgical Endoscopy*, vol. 16, no. 10, pp. 1389–1402, Mar. 2002.
- [6] U. Rembold and C. Burghart, "Surgical robotics: An introduction," *Journal of Intelligent and Robotic Systems*, vol. 30, pp. 1–28, Mar. 2001.
- [7] M. Ferre, M. Buss, R. Aracil, C. Melchiorri, and C. Balaguer, *Introduction to Advances in Telerobotics*. Springer Berlin Heidelberg, 2007, vol. 31.
- [8] J. Lloyd, J. Beis, D. Pai, and D. Lowe, "Model-based telerobotics with vision," in *IEEE International Conference on Robotics and Automation*, Albuquerque, NM, Apr. 1997, pp. 1297–1304.
- [9] C. Preusche and G. Hirzinger, "Haptics in telerobotics: Current and future research applications," *The Visual Computer: International Journal of Computer Graphics*, vol. 23, no. 4, pp. 273–284, Mar. 2007.
- [10] N. Rodríguez, J.-P. Jessel, and P. Torguet, "A virtual reality tool for teleoperation research," *Virtual Reality*, vol. 6, no. 2, pp. 57–62, Sept. 2002.
- [11] G. Mageses, J. Vercher, and G. Gauthier, "Hand movement strategies in telecontrolled motion along 2-D trajectories," *IEEE Transactions on Systems, Man, and Cybernetics*, vol. 22, no. 2, pp. 242–257, Apr. 1992.
- [12] A. A. Maciejewski and C. A. Klein, "Obstacle avoidance for kinematically redundant manipulators in dynamically varying environments," *International Journal of Robotics Research*, vol. 4, no. 3, pp. 109–117, 1985.
- [13] A. A. Maciejewski and C. A. Klein, "The singular value decomposition: Computation and applications to robotics," *International Journal of Robotics Research*, vol. 8, no. 6, pp. 63–79, 1989.
- [14] R. G. Roberts and A. A. Maciejewski, "A local measure of fault tolerance for kinematically redundant manipulators," *IEEE Transactions on Robotics and Automation*, vol. 12, no. 4, pp. 543–552, Aug. 1996.
- [15] R. C. Hoover, R. G. Roberts, and A. A. Maciejewski, "Implementation issues in identifying the failure-tolerant workspace boundaries of a kinematically redundant manipulators," in *Proc. IEEE International Conference on Intelligent Robots and Systems*, San Diego, CA, Oct./Nov 2008, pp. 3528–3533.
- [16] R. Marin, P. Sanz, and J. Sanchez, "A very high level interface to teleoperate a robot via web included augmented reality," in *IEEE International Conference on Robotics and Automation*, Washington, DC, May 2002, pp. 2725–2730.
- [17] W.-K. Yoon, Y. Tsumaki, and M. Uchiyama, "An experimental system for dual-arm robot teleoperation in space with concepts of virtual grip and ball," in *International Conference on Advanced Robotics*, Tokyo, Japan, Oct. 1999, pp. 225–230.
- [18] M. Goel, "Tolerating undetected failures in robotic manipulators," Ph.D. dissertation, Purdue University, Dec. 1998.
- [19] M. Goel, A. Maciejewski, V. Balakrishnan, and R. Proctor, "Failure tolerant teleoperation of a kinematically redundant manipulator: An experimental study," *IEEE Transactions on Systems, Man, and Cybernetics*, vol. 33, no. 6, Nov. 2003.